

Raman Spectroscopic Assessment of Myocardial Viability in Langendorff-Perfused Ischemic Rat Hearts

**Koki Ikemoto^{1,2}, Kosuke Hashimoto^{1,5}, Yoshinori Harada¹, Yasuaki Kumamoto^{1,6},
Michiyo Hayakawa¹, Kentaro Mochizuki¹, Kazuhiko Matsuo³, Kenta Yashiro³,
Hitoshi Yaku², Tetsuro Takamatsu⁴ and Hideo Tanaka¹**

¹Department of Pathology and Cell Regulation, Graduate School of Medical Science, Kyoto Prefectural University of Medicine, 465 Kajii-cho Kamigyo-ku, Kyoto 602–8566, Japan, ²Department of Cardiovascular Surgery, Graduate School of Medical Science, Kyoto Prefectural University of Medicine, 465 Kajii-cho Kamigyo-ku, Kyoto 602–8566, Japan, ³Department of Anatomy and Developmental Biology, Graduate School of Medical Science, Kyoto Prefectural University of Medicine, 465 Kajii-cho Kamigyo-ku, Kyoto 602–8566, Japan, ⁴Department of Medical Photonics, Kyoto Prefectural University of Medicine, 465 Kajii-cho Kamigyo-ku, Kyoto 602–8566, Japan, ⁵Present address: Department of Biomedical Chemistry, School of Science and Technology, Kwansai Gakuin University, Gakuen, Hyogo 669–1337, Japan and ⁶Present address: Department of Applied Physics, Graduate School of Engineering, Osaka University, Osaka 565–0871, Japan

Received February 3, 2021; accepted March 5, 2021; published online April 17, 2021

Spontaneous Raman spectroscopy, which senses changes in cellular contents of reduced cytochrome c, could be a powerful tool for label-free evaluation of ischemic hearts. However, undetermined is whether it is applicable to evaluation of myocardial viability in ischemic hearts. To address this issue, we investigated sequential changes in Raman spectra of the subepicardial myocardium in the Langendorff-perfused rat heart before and during ligation of the left coronary artery and its subsequent release and re-ligation. Under 532-nm wavelength excitation, the Raman peak intensity of reduced cytochrome c at 747 cm⁻¹ increased quickly after the coronary ligation, and reached a quasi-steady state within 30 min. Subsequent reperfusion of the heart after a short-term (30-min) ligation that simulates reversible conditions resulted in quick recovery of the peak intensity to the baseline. Further re-ligation resulted in resurgence of the peak intensity to nearly the identical value to the first ischemia value. In contrast, reperfusion after prolonged (120-min) ligation that assumes irreversible states resulted in incomplete recovery of the peak intensity, and re-ligation resulted in inadequate resurgence. Electron microscopic observations confirmed the spectral findings. Together, the Raman spectroscopic measurement for cytochrome c could be applicable to evaluation of viability of the ischemic myocardium without labeling.

Key words: Raman spectroscopy, myocardial viability, ischemia, cytochrome c, mitochondria

I. Introduction

Occlusion of the coronary arterial blood flow renders the downstream myocardium ischemic, i.e., it shows sub-

stantial depletions of the oxygen delivery and metabolic substrate, resulting in immediate drop in contractile performance due to cessations of the mitochondrial oxidative phosphorylation and adenosine triphosphate (ATP) synthesis [16]. As long as the coronary occlusion persists, ischemic injury of the myocardium progresses over time with concomitant biochemical and ultrastructural changes in the mitochondria [18]. After a long period of ischemia, the myocardium eventually loses its viability, where the

Correspondence to: Yoshinori Harada, Department of Pathology and Cell Regulation, Graduate School of Medical Science, Kyoto Prefectural University of Medicine, 465 Kajii-cho Kamigyo-ku, Kyoto 602–8566, Japan. E-mail: yoharada@koto.kpu-m.ac.jp

injury is rendered irreversible even after the coronary flow is resumed [3].

Evaluation of ischemic myocardial viability, i.e., whether ischemia-damaged myocardium recovers function after restoration of the coronary perfusion [9, 11, 38], is essential to determine the most suitable procedures of cardiac surgery for patients with ischemic heart disease. Accurate coronary artery bypass grafting (CABG) to the viable myocardium and proper excision of non-viable myocardium by surgical ventricular restoration (SVR) critically determine the postoperative outcomes for the heart surgery [11, 38]. However, evaluation of myocardial viability for determining the surgical procedures has hitherto been performed only by limited modalities, i.e., myocardial scintigraphy and gadolinium-enhanced magnetic resonance imaging, both of which are utilized only preoperatively and not available for precise intraoperative evaluation [11, 38]. Regarding this issue, Raman spectroscopic analysis may be a promising candidate, which provides clues to identify the molecular structure of substances without using any specific chemical labeling, e.g., by fluorescent dyes [14, 15, 17, 21, 29, 33]: specific Raman shifts in Raman spectrum acquired under green light excitation can be used to unveil changes of molecules such as reduced cytochromes c and b, oxygenated myoglobin and lipids [1, 6, 20, 31]. We have previously demonstrated that myocardial ischemia and infarct could be detected quantitatively by Raman scattering light, which represents the energy states of molecular vibrations [26, 27, 37]. We have also demonstrated that Raman spectroscopy enables label-free evaluation of ischemic conditions in global, stopped-flow ischemia models of Langendorff-perfused rat hearts; the spectral peak of reduced cytochromes c at 747 cm^{-1} reveals subtle ischemic changes, which arise before the emergence of the morphological changes in hematoxylin-eosin (H & E) histology or di-4-ANEPPS fluorescence images of membrane structures, mitochondrial functional states evaluated by 2,3,5-triphenyltetrazolium chloride (TTC) staining, and mitochondrial membrane potentials by tetramethyl rhodamine ethyl ester (TMRE) fluorescence intensity [28]. However, undetermined is applicability of Raman spectroscopic measurements to assess whether the ischemic myocardium resumes its functions after re-establishment of the coronary arterial perfusion.

In this study, we assumed that coronary arterial occlusion and subsequent reperfusion exhibits quick and reversible changes in the Raman spectrum for reduced cytochrome c under viable conditions, whereas the non-viable conditions fail to show reversible changes in the spectra by repetition of occlusion/reperfusion procedures. To address this assumption, we sought to measure the Raman spectral changes in Langendorff-perfused rat hearts under ischemic conditions induced by the left coronary arterial ligation for 30 min or 120 min and subsequent reperfusion and re-ligation. The aim of our study was to evaluate myocardial viability by Raman spectroscopy.

II. Materials and Methods

Heart preparation

Our animal experiments were conducted in accordance with *the Guide for the Care and Use of Laboratory Animals* (8th edition, Washington DC: National Academies Press (US); 2011) and performed under approval of the Animal Research Committee, Kyoto Prefectural University of Medicine. Under deep general anesthesia of Wistar rats (male, 200–300 g) with a combination of three anesthetic agents, namely medetomidine, midazolam, and butorphanol [19], we rapidly excised the hearts after medial sternotomy and subsequent injection of heparin (1 U/g body weight) via the inferior vena cava. Retrograde perfusion was provided via the aorta with oxygenated Tyrode's solution containing (in mM) NaCl 145, KCl 5.4, MgCl_2 1, CaCl_2 1, glucose 10, HEPES 10, and NaHPO_4 0.33 (pH 7.4 adjusted with NaOH at 37°C) at a constant flow rate of 10–12 mL/min controlled by a micro tube pump (MP-3N, Tokyo Rikakikai, Japan). We placed the heart with its anterior wall upward on a dedicated chamber maintained at 37°C by a Peltier control system.

Model of local ischemia

Following the initial perfusion of the heart with Tyrode's solution for 30 min to stabilize its redox state [24], we performed continuous perfusion with Tyrode's solution with 20 mM 2,3-butanedione monoxime (BDM) (Nacalai Tesque, Japan) added to attenuate the contraction [13]. The complete ligation of the left descending coronary artery at a site just before the bifurcation of a diagonal branch (Fig. 1A), induced local ischemia for 30 min in some experiments (30-min ligation; $n = 5$) and 120 min in others (120-min ligation; $n = 8$). After the first ligation for 30 min or 120 min, we re-perfused the coronary artery for 20 min by release of the ligature. The second ischemia was induced for the following 30-min ligation in a similar manner (Fig. 1B). The anterior wall of the left ventricle was divided into perfused and non-perfused (i.e., ischemic) areas (Fig. 1A). In some experiments, 0.5% Evans blue-containing phosphate-buffered saline was perfused for assessment of the coronary arterial circulation.

Measurement of Raman spectra

We used a slit-scanning laser Raman confocal microscope (Nanophoton, Osaka, Japan) that is described in the previous work [28]. The excitation wavelength of the frequency doubled Nd: YAG laser was 532 nm; the laser was focused into a line-shaped beam at the sample with an objective lens (UPLSAPO 10X, NA = 0.30, Olympus, Tokyo, Japan). The sample excitation intensity was set to $13.8\ \mu\text{W}/\mu\text{m}^2$. The backward Raman scattering from the line illumination was collected with the same objective lens and then was guided into the entrance slit of a Czerny–Turner spectrograph ($f = 500\text{ mm}$) equipped with a blazed grating having 600 g/mm groove density. The slit width

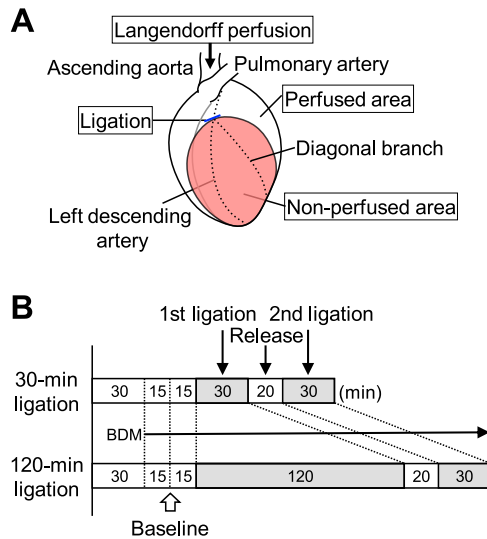


Fig. 1. Experimental schematic diagram and time course. **(A)** An isolated heart is perfused retrogradely from the ascending aorta. The left descending artery is ligated just before the bifurcation of the diagonal branch. The left ventricular wall is divided into perfused and non-perfused areas. **(B)** The 1st ischemia is created by 30-min or 120-min coronary arterial ligation. Durations of baseline perfusion, reperfusion, and the 2nd ligation phases are 60, 20, and 30 min, respectively, in both models. BDM, 2,3-butanedione monoxime.

was set at 100 μm . The scattered light was dispersed by a 600-groove/mm grating, and the Raman spectra were acquired with a cooled CCD camera (1340 \times 400 pixels, PIXIS 400BR, Princeton Instruments, Trenton, NJ, USA). The exposure time for each acquisition was 10 sec. The spectra, collected from two random lines (1.6-mm length), were averaged, and subsequently served for spectral analysis. All raw Raman spectra were calibrated using the known lines of ethanol. We recorded Raman spectra from non-perfused (i.e., ischemic) and perfused (i.e., non-ischemic) areas, at both 15 and 30 min after commencement of the coronary perfusion of the BDM-containing Tyrode's solution (Fig. 1B). We also collected the spectra during the first ischemic, re-perfused, and second ischemic phases at each scheduled time point in both models.

Data processing of Raman spectra

The spectra having the calibrated axis were interpolated with a third-order splined function. We employed the open source algorithm developed by Zhang *et al.* with R (version 3.5.2) to remove the fluorescent background [39]. The spectra were then smoothed with Savitzky-Golay filtering and normalized with the intensity of the CH deformation band at 1447 cm^{-1} .

Electron microscopy

We fixed the hearts after the first ischemic phase with 2% paraformaldehyde and 2% glutaraldehyde at 4°C overnight. The tissue samples were cut to about three mm square followed by post-fixation with 1% osmium tetroxide

in 0.1 M phosphate buffer. They were then dehydrated in a series of graduated ethanol solutions (50%, 60%, 70%, 80%, 90%, 99.6% and 100%, three times for each) at room temperature for 20 min each. Dehydrated samples were immersed into the half Epon (1:1 resin:ethanol mixture) overnight, followed by full Epon for an hour twice. We eventually obtained the solid pellet by embedding the samples into epoxy resin (Poly/Bed 812) at 60°C for 48 hr. An ultramicrotome equipped with a diamond knife set at 70 nm for the preparation of single section or serial sections was used to obtain ultra-thin sections. We collected these sections onto formvar-coated grids and stained them with EM stainer (Nisshin EM, Tokyo, Japan). We observed the cross-section samples using a transmission electron microscope (JEM-1220, JEOL, Tokyo, Japan) at the end of the first ischemic phase [34].

TTC staining

The perfused hearts were cut parallel to the short axis into 5 slices (approx. 2-mm thickness) after 30-min and 120-min coronary arterial ligation. The slices were incubated in 1% 2,3,5-triphenyltetrazolium chloride (TTC) in 0.1 M phosphate-buffered solution for 30 min at 37°C, and imaged by using a vital light microscope (SZX12, Olympus, Tokyo, Japan).

Enzymatic activity analysis

We examined the enzymatic activities of mitochondrial oxidative phosphorylation using a complex I enzyme activity microplate assay kit (ab109721, Cambridge, UK) and a complex IV rodent enzyme activity microplate assay kit (ab109911) (Supplementary Fig. S2A). Tissue homogenates were used for the analysis obtained from the left ventricular myocardium after Langendorff perfusion under the following conditions: perfused and non-perfused areas of 30-min ligation model and perfused and non-perfused areas of 120-min ligation model. We measured the optical density (OD) using a Synergy H1 microplate reader (BioTek Japan, Tokyo, Japan).

Western blot analysis

Western blot analysis was performed as previously reported [32]. We extracted total proteins from the following Langendorff-perfused heart tissues to examine the protein level of NDUFB8, cytochrome c, and COX4I1: specimens without coronary ligation termed as “baseline”, perfused and nonperfused areas of 30-min ligation model, and perfused and nonperfused areas of 120-min ligation model. The extracted proteins were separated by 10% SDS-PAGE and transferred to a PVDF membrane (IPVH09120, Merck, Darmstadt, Germany). The membranes were blocked with 5% skim milk, followed by an incubation with NDUFB8 antibody (459210, Thermo Fisher Scientific) or cytochrome c (ab133504, Abcam), COX4I1 (11242-1-AP, Proteintech, IL, USA), and GAPDH (016-25523, Wako, Osaka, Japan). The cytochrome c anti-

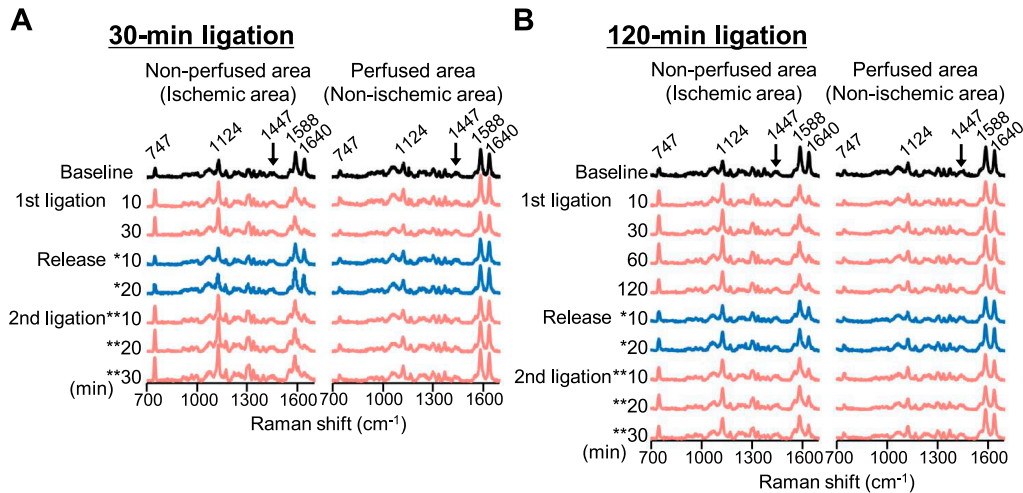


Fig. 2. Sequential representations of averaged Raman spectra. Averaged Raman spectra acquired from the surface of perfused rat hearts at ischemic (non-perfused) and non-ischemic (perfused) areas of the 30-min (**A**) and 120-min (**B**) ligation models at each time point. * and ** denote the time points after commencement of reperfusion and 2nd ligation, respectively.

body recognizes both the reduced and oxidized forms. The membranes were incubated with a secondary antibody conjugated with HRP (anti-mouse IgG: AP200P, Merck, anti-rabbit IgG: 100064301, Cayman Chemical, MI, USA). The immunoreactive bands were detected by ImmunoStar[®] Zeta (Wako) (Supplementary Fig. S2B).

Assessment of the superficial circulation by Evans blue dye

To address to what extent the microcirculation is impaired by stopped flow ischemia, we observed the surface of the Langendorff-perfused rat hearts after perfusion of 0.5% Evans blue (Nacalai, Kyoto, Japan) in phosphate buffered saline using a white-light microscope (SZX12; Olympus), equipped with a color CCD digital camera (DP70; Olympus) (Supplementary Fig. S3).

Statistical analysis

Quantitative data are presented as the mean plus/minus standard deviation. We used the nonparametric Mann-Whitney U test to analyze continuous variables. A p -value < 0.05 was considered statistically significant. All statistical calculations were performed using SPSS version 24.0 software (SPSS Inc., Chicago, IL, USA).

III. Results

Raman spectra

Fig. 2 shows sequential changes in the Raman spectra in the subepicardial myocardium of the Langendorff-perfused rat heart before, during coronary-artery ligation, and during its subsequent release and re-ligation. After confirmation of the overall Raman spectra being stable for 15 min (shown as “baseline”), the peaks at 747 cm^{-1} and 1124 cm^{-1} , regarded as reduced cytochrome c and b respectively [2, 26, 27], exhibited a quick elevation in the non-perfused

(i.e., ischemic) region induced by the ligation within 10 min, and reached a quasi-steady state within 30 min (Fig. 2A). Continuation of the ligation up to 120 min also maintained highly-stable values for these two peaks (Fig. 2B). It should also be noted that even during the ligation period, the Raman spectra at the intact region (i.e., under continuously perfused area) exhibited no apparent changes in the spectral waveforms, supporting the notion that the augmentation of the peaks at 747 cm^{-1} and 1124 cm^{-1} were due to the absence of the coronary flow. Following reperfusion, the peaks at 747 cm^{-1} and 1124 cm^{-1} were restored to the baseline level after 30-min ligation, and these exhibited an immediate elevation again by re-ligation (Fig. 2A). In contrast, during reperfusion after 120-min occlusion the peak values at 747 cm^{-1} and 1124 cm^{-1} appeared incompletely reduced to the baseline, and the values regained insufficiently by re-occlusion (Fig. 2B). In addition, the bands at 1588 and 1640 cm^{-1} , assigned as oxygenated myoglobin [2], were also responsive to ischemia and reperfusion and showed reverse trends compared with those at 747 and 1124 cm^{-1} (Fig. 2).

The observed different responses to the Raman peaks by reperfusion and re-occlusion between the 30-min and 120-min coronary occlusions may indicate differences in the redox reactions of cytochromes and myoglobin. However, the peak absolute values of these 4 wave numbers, showing no steady state after ligation, may include certain progressive “background” despite subtraction of the background. Focusing here on the relatively constant value at 1447 cm^{-1} , reflecting C-H bending of lipids [7, 23], we standardized the peak values at 747 , 1124 , 1588 , and 1640 cm^{-1} by calculating the ratio of the individual peak intensities divided by the corresponding peaks at 1447 cm^{-1} (I_{747}/I_{1447} , I_{1124}/I_{1447} , I_{1588}/I_{1447} , and I_{1640}/I_{1447}) as a reference for precise evaluation of the peaks (Fig. 3 and

Supplementary Fig. S1). Of the 4 different peaks demonstrated above, we focused on the most sensitive Raman spectrum, at 747 cm^{-1} , which is assigned as the reduced cytochrome c content, represent the redox activity of the mitochondria [2, 28]. As shown in Fig. 3, the I_{747}/I_{1447} values increased rapidly after the induction of coronary ligation in the ischemic (non-perfused) area of 30-min and 120-min ligation models. The ratio reached a quasi-steady state at about 30 min. After reperfusion, the ratios promptly decreased to the baseline level. However, the value in the 120-min ligation failed to completely drop to the baseline (Fig. 3B and 3C). The ratio I_{747}/I_{1447} in the 30-min ligation showed a rapid increase during the second ischemic phase and reached a plateau as high as that in the first phase. In contrast, there was no significant increase in the 120-min occlusion (Fig. 3A, 3B, and 3C). These responses may indicate an impairment of the mitochondrial redox function in the non-perfusion area of the 120-min occlusion. The other 3 peak values, I_{1124}/I_{1447} , I_{1588}/I_{1447} , and I_{1640}/I_{1447} , also showed similar time courses; however, the changes appeared ambiguous as compared with I_{747}/I_{1447} in both models (Supplementary Fig. S1).

Histochemical and morphological evaluations

Given that the Raman spectral changes indicate depressed mitochondrial functions by the second trial of the coronary ligation, we compared the TTC stainability of ischemic heart after 30-min and 120-min coronary artery ligation. As expected, the heart after 120-min ligation was barely stained with TTC at the non-perfused area, whereas the 30-min ligated heart was uniformly stained at the perfused and non-perfused areas (Fig. 4A), indicating an impairment of the electron transport chain (ETC) complex II function [8, 22]. However, there was no significant differences in protein expressions and enzyme activities for complexes I and IV between the 30-min and 120-min ligation models (Supplementary Fig. S2A and S2B).

Morphologically, however, the H & E stained, light microscopic images of the heart indicate no apparent difference between the 30-min and 120-min ischemic myocardium (Fig. 4B). However, definitive ultrastructural changes were observed in the myocardium especially on 120-min occlusion by electron microscopy. As shown in Fig. 4C, the heart after 30-min ligation revealed that sarcomere structures of the cardiomyocytes were well preserved with clear Z bands of the myofibrils identified in both the perfusion and non-perfusion (i.e., ischemic) areas. In addition, the mitochondria were located along the sarcomeres with densely packed cristae. In sharp contrast, the 120-min ischemia appeared to impair the mitochondrial structure, particularly that of the inner membrane. The mitochondria were swollen with abundant amorphous matrices. The outer membrane of the mitochondria was preserved; however, cristae were partially disrupted. The ischemic region of the 120-min ligation was edematous for sarcomeres with unclear boundary of the Z bands.

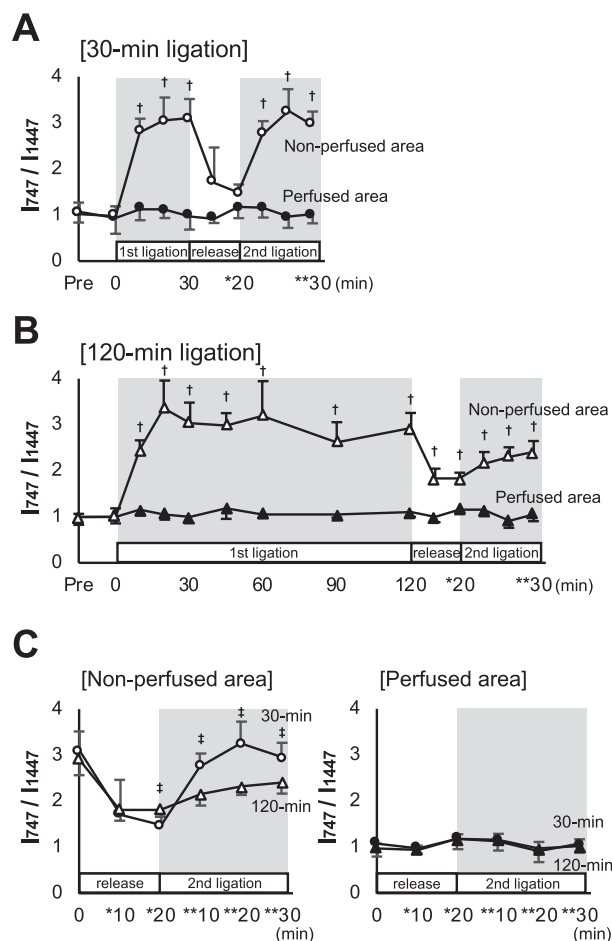


Fig. 3. Sequential changes in Raman spectral peak intensity ratio. Graphs plotting ratios of the peak values at 747 cm^{-1} over those at 1447 cm^{-1} (I_{747}/I_{1447}) throughout the experiment in 30-min (A) and 120-min (B) ligation models. (C) Graphs comparing Raman spectral peak ratios during reperfusion after 30-min and 120-min 1st ligation and the 2nd ligation phase at perfused and non-perfused areas. * and ** denote the time points after commencement of reperfusion and 2nd ligation, respectively. † denotes $P < 0.05$ using the nonparametric Mann-Whitney U test between perfused and non-perfused areas corresponding to the same time. ‡ denotes $P < 0.05$ by the same analysis as above between 30-min and 120-min ligation at each time point. Data are presented as mean \pm SD.

IV. Discussion

In this study, we demonstrated that the Raman spectral peak intensity at 747 cm^{-1} , a reflection of the cytochrome c, is reversibly increased and decreased in short-term (30 min) ligation of the coronary artery and its release respectively, and that re-ligation again increased the peak level to the same degree as the first ones. By contrast, the reperfusion and the second ligation after the long-term (120-min) ischemia impaired the spectral responses. In accordance with these observations, the ultrastructure of the myocardium showed no discernible changes after the short-term ischemia, while irreversible mitochondrial damage was observed after the prolonged ischemia. These observa-

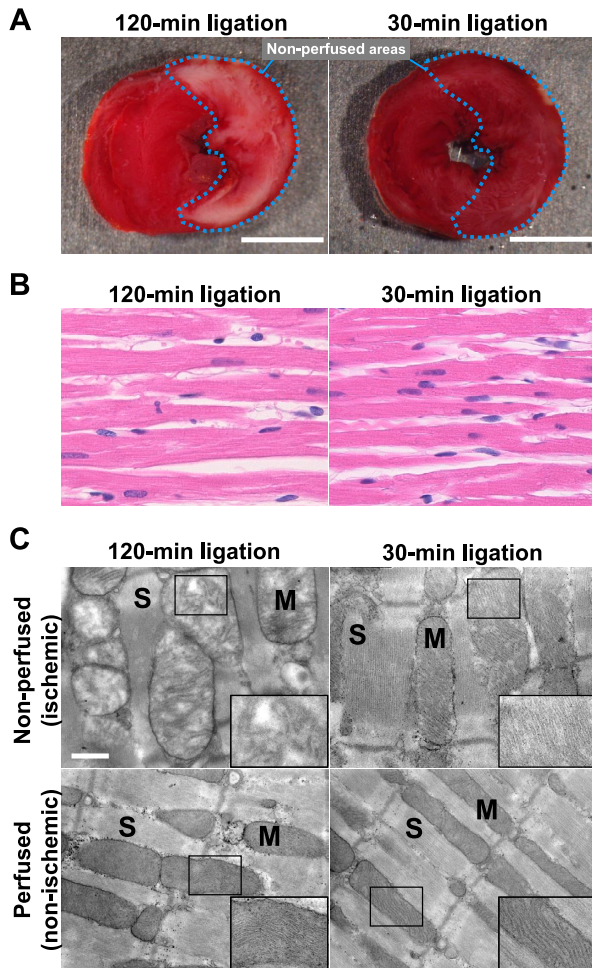


Fig. 4. Comparison between the non-perfused (ischemic) areas of the heart at the end of the first ischemic phases in 30-min and 120-min ligation models. **(A)** Triphenyl tetrazolium chloride-stained hearts. Putative non-perfused areas are indicated by the dotted line. Bar = 5 mm. **(B)** H & E-stained images of the ischemic myocardium. **(C)** Ultrastructural details of cardiomyocytes in perfused and non-perfused areas. For references, the images obtained from perfused areas are also shown (bottom). The insets are magnified images of mitochondria. Electron micrograph, $\times 15000$. Bar = 500 nm. M, mitochondria; S, sarcomere.

tions indicate that the Raman spectroscopy has potential for determining viability of ischemic myocardium after restoration of the coronary arterial flow.

The quick and remarkable increase in the 747 cm^{-1} Raman peak intensity in the early ischemia phase can be attributed to the failure to oxidize cytochrome *c* by complex IV at the final step of the ETC, because of the insufficient oxygen supply. The complete and second quick recovery of the 747 cm^{-1} peak intensity by reperfusion and the rapid resurgence by the second ischemic trial would be explained by the immediate oxidization and reduction of cytochrome *c*. These reversible responses indicate that the mitochondrial electron transport function is preserved in the 30-min ischemic myocardium. In other words, the myocardium can be viable. The increase in the

reduced cytochrome *c* by re-ligation is unlikely to involve ischemic preconditioning effect of the first 30-min ligation, because the re-ligation faithfully regained the peak nearly identically to that induced by the first ligation; according to our previous experiments, the preconditioning effect was observed after repetition of brief periods (2 min) of ischemia/reperfusion [37].

The inadequate reversibility of the intensity peak after the 120-min ischemia, reflecting impaired oxidoreduction process of cytochrome *c*, would not be due to impaired reperfusion of the coronary circulation: the Evans blue images showed well-preserved perfusion even after release of the 120-min ligation (Supplementary Fig. S3). Reduced activity of succinate dehydrogenase by electron transport chain complex II would be responsible for the poor reversibility of the 747 cm^{-1} peak intensity in the hearts after the 120-min ischemia because of the reduced TTC staining of the heart (Fig. 4A) [8, 22]. Reduced activities of complex I or complex IV would not account for the irreversible, low viability conditions of the myocardium, because of the absence of apparent changes in these enzymatic activities (Supplementary Fig. S2).

We found that the mitochondria in the 120-min ischemic myocardium were swollen with their inner membrane structures partially collapsed, whereas the 30-min ischemic myocardium showed no obvious morphological changes, with the inner membrane structure well maintained (Fig. 4B). These findings indicate that the electron transport function and mitochondrial membrane potential were impaired in the 120-min ischemia, but not in the 30-min ischemia. In other words, the mitochondria in the 120-min ischemic myocardium were irreversibly injured. Our observations are in good agreement with previous ultrastructural studies in dog hearts: the mitochondria of the intact and reversibly injured myocytes were densely packed with cristae, whereas those of irreversible ones were swollen and exhibited a distorted arrangement of cristae [18]. The irreversible ischemic injury results in a loss of mitochondrial membrane potentials via the opening of mitochondrial permeability transition pore [25], which results in cessation of ATP synthesis, influx of solute, and swelling of mitochondria [12, 36]. We have previously demonstrated that the TMRE fluorescence-based mitochondrial membrane potential is rapidly lost about 37 min after the globally stopped flow of the coronary arteries [28]. Given that the 37-min ischemia is a critical period of no return, our present ultrastructural observations of mitochondria are reasonable to explain the difference in Raman spectral changes between the two different-period ligation models. However, it should be noted that our experimental results are not always consistent with the clinical data. In practice, patients with myocardial infarction who received early coronary arterial reperfusion within 90 min showed good clinical outcomes [10, 35], therefore, it is conceivable that the critical period of no return in ischemic human hearts may be longer than that in the ischemic rat hearts we

studied. We assume that the discrepancy is due to the differences between experimental and clinical conditions, e.g., presence or absence of the blood and/or species differences.

Our study has some limitations. First, we conducted experiments by using blood-free perfusates. Second, the mechanical contraction was intentionally suppressed by BDM to accurately capture the Raman spectra of the heart. Such non-physiological experimental conditions as conducted here for simplicity's sake may well have hampered valid evaluation of the genuine myocardial viability. Further evaluation is mandatory under blood perfused, BDM-free conditions. Third, our evaluation was limited only on the subepicardial myocardium less affected by coronary insufficiency as compared with the mid or subendocardial myocardium. We probed at the depth of 50 μm beneath the epicardium, where the Raman signal was most efficiently obtained from the surface. We assume that the Raman spectroscopic signal detection using 532-nm excitation would be restricted to $\sim 100\text{-}\mu\text{m}$ deep from the surface due to the unavoidable factors in the myocardium, e.g., light absorbance and scattering efficiency [4, 30]. Despite these limitations, however, it would be safe to assume that the spontaneous Raman spectroscopy is applicable to a straightforward assessment of the viability of ischemic myocardium.

In conclusion, our study suggests that Raman spectroscopy can be used to evaluate the viability of ischemic myocardium under label-free conditions. As far as we know, clinical application of Raman spectroscopy to cardiovascular diseases has not been achieved. Recent clinical studies show that Raman spectroscopy is applicable to the diagnosis of malignant tumors [4, 5], although they are still in the developing stage. Our approaches would highlight the potential of Raman spectroscopy for the treatment of ischemic heart disease.

V. Conflicts of Interest

Yoshinori Harada and Tetsuro Takamatsu have a patent JP5372137B2 issued to Tetsuro Takamatsu, Mitsugu Ogawa, Yoshinori Harada, and a patent P6103700 issued to Tetsuro Takamatsu, Yoshinori Harada, Takeo Minamikawa, Nanae Muranishi, Katsuhiro Ishii, Juichiro Ukon, Junichi Aoyama. The other authors have nothing to disclose.

VI. Acknowledgments

This work was supported by the Japan Society for the Promotion of Science [JP16K01366]; and the Japan Science and Technology Agency [JPMJCR1662].

VII. References

1. Adar, F. and Erecinska, M. (1974) Resonance Raman spectra of the b- and c-type cytochromes of succinate-cytochrome c

- reductase. *Arch. Biochem. Biophys.* 165; 570–580.
2. Brazhe, N. A., Treiman, M., Brazhe, A. R., Find, N. L., Maksimov, G. V. and Sosnovtseva, O. V. (2012) Mapping of redox state of mitochondrial cytochromes in live cardiomyocytes using Raman microspectroscopy. *PLoS One* 7; e41990.
3. Carmeliet, E. (1984) Myocardial ischemia: reversible and irreversible changes. *Circulation* 70; 149–151.
4. Chaichi, A., Prasad, A. and Gartia, M. R. (2018) Raman Spectroscopy and Microscopy Applications in Cardiovascular Diseases: From Molecules to Organs. *Biosensors (Basel)* 8; 107.
5. Cordero, E., Latka, I., Matthäus, C., Schie, I. W. and Popp, J. (2018) In-vivo Raman spectroscopy: from basics to applications. *J. Biomed. Opt.* 23; 071210.
6. Czamara, K., Majzner, K., Pacia, M. Z., Kochan, K., Kaczor, A. and Baranska, M. (2015) Raman spectroscopy of lipids: a review. *J. Raman Spectrosc.* 46; 4–20.
7. Davidson, B., Murray, A. A., Elfick, A. and Spears, N. (2013) Raman micro-spectroscopy can be used to investigate the developmental stage of the mouse oocyte. *PLoS One* 8; e67972.
8. Dhingra, R. and Kirshenbaum, L. (2015) Succinate dehydrogenase/complex II activity obligatorily links mitochondrial reserve respiratory capacity to cell survival in cardiac myocytes. *Cell Death Dis.* 6; e1956–e1956.
9. Dilsizian, V. (1996) Myocardial viability: Contractile reserve or cell membrane integrity? *J. Am. Coll. Cardiol.* 28; 443–446.
10. Foo, C. Y., Bonsu, K. O., Nallamothu, B. K., Reid, C. M., Dhipayom, T., Reidpath, D. D., et al. (2018) Coronary intervention door-to-balloon time and outcomes in ST-elevation myocardial infarction: a meta-analysis. *Heart* 104; 1362–1369.
11. Gewirtz, H. and Dilsizian, V. (2017) Myocardial viability: survival mechanisms and molecular imaging targets in acute and chronic ischemia. *Circ. Res.* 120; 1197–1212.
12. Goldenthal, M. J. (2016) Mitochondrial involvement in myocyte death and heart failure. *Heart Fail. Rev.* 21; 137–155.
13. Habazettl, H., Palmisano, B. W., Bosnjak, Z. J. and Stowe, D. F. (1996) Initial reperfusion with 2,3 butanedione monoxime is better than hyperkalemic reperfusion after cardioplegic arrest in isolated guinea pig hearts. *Eur. J. Cardiothorac. Surg.* 10; 897–904.
14. Harada, Y., Dai, P., Yamaoka, Y., Ogawa, M., Tanaka, H., Nosaka, K., et al. (2009) Intracellular dynamics of topoisomerase I inhibitor, CPT-11, by slit-scanning confocal Raman microscopy. *Histochem. Cell Biol.* 132; 39–46.
15. Hashimoto, M. (2002) Coherent anti-Stokes Raman scattering microscopy. *Acta Histochem. Cytochem.* 35; 83–86.
16. Hearse, D. J. (1979) Oxygen deprivation and early myocardial contractile failure: a reassessment of the possible role of adenosine triphosphate. *Am. J. Cardiol.* 44; 1115–1121.
17. Helal, K. M., Taylor, J. N., Cahyadi, H., Okajima, A., Tabata, K., Itoh, Y., et al. (2019) Raman spectroscopic histology using machine learning for nonalcoholic fatty liver disease. *FEBS Lett.* 593; 2535–2544.
18. Jennings, R. B. and Reimer, K. A. (1981) Lethal myocardial ischemic injury. *Am. J. Pathol.* 102; 241–255.
19. Kawai, S., Takagi, Y., Kaneko, S. and Kurosawa, T. (2011) Effect of three types of mixed anesthetic agents alternate to ketamine in mice. *Exp. Anim.* 60; 481–487.
20. Kitagawa, T., Kyogoku, Y., Iizuka, T. and Saito, M. I. (1976) Nature of the iron-ligand bond in ferrous low spin hemoproteins studied by resonance Raman scattering. *J. Am. Chem. Soc.* 98; 5169–5173.
21. Kumamoto, Y., Harada, Y., Takamatsu, T. and Tanaka, H. (2018) Label-free Molecular Imaging and Analysis by Raman Spectroscopy. *Acta Histochem. Cytochem.* 51; 101–110.
22. Kun, E. and Abood, L. (1949) Colorimetric estimation

- of succinic dehydrogenase by triphenyltetrazolium chloride. *Science* 109; 144–146.
23. Managò, S., Valente, C., Mirabelli, P., Circolo, D., Basile, F., Corda, D., *et al.* (2016) A reliable Raman-spectroscopy-based approach for diagnosis, classification and follow-up of B-cell acute lymphoblastic leukemia. *Sci. Rep.* 6; 1–13.
 24. Matsumoto-Ida, M., Akao, M., Takeda, T., Kato, M. and Kita, T. (2006) Real-time 2-photon imaging of mitochondrial function in perfused rat hearts subjected to ischemia/reperfusion. *Circulation* 114; 1497–1503.
 25. Maximilian Buja, L. (2017) Mitochondria in Ischemic Heart Disease. vol. 982, *Advances in Experimental Medicine and Biology*, Springer, Cham. pp. 127–140.
 26. Nishiki-Muranishi, N., Harada, Y., Minamikawa, T., Yamaoka, Y., Dai, P., Yaku, H., *et al.* (2014) Label-free evaluation of myocardial infarction and its repair by spontaneous Raman spectroscopy. *Anal. Chem.* 86; 6903–6910.
 27. Ogawa, M., Harada, Y., Yamaoka, Y., Fujita, K., Yaku, H. and Takamatsu, T. (2009) Label-free biochemical imaging of heart tissue with high-speed spontaneous Raman microscopy. *Biochem. Biophys. Res. Commun.* 382; 370–374.
 28. Ohira, S., Tanaka, H., Harada, Y., Minamikawa, T., Kumamoto, Y., Matoba, S., *et al.* (2017) Label-free detection of myocardial ischaemia in the perfused rat heart by spontaneous Raman spectroscopy. *Sci. Rep.* 7; 42401.
 29. Raman, C. V. and Krishnan, K. S. (1928) A new type of secondary radiation. *Nature* 121; 501.
 30. Sikurova, L., Habodászová, D., Gonda, M., Waczulíková, I. and Vojtek, P. (2003) Penetration of laser light through blood derivatives. *Laser Phys.* 13; 217–221.
 31. Spiro, T. G. and Streckas, T. C. (1972) Resonance Raman spectra of hemoglobin and cytochrome c: inverse polarization and vibronic scattering. *Proc. Natl. Acad. Sci. USA* 69; 2622–2626.
 32. Takeda, Y., Harada, Y., Yoshikawa, T. and Dai, P. (2017) Direct conversion of human fibroblasts to brown adipocytes by small chemical compounds. *Sci. Rep.* 7; 4304–4304.
 33. Taylor, J. N., Mochizuki, K., Hashimoto, K., Kumamoto, Y., Harada, Y., Fujita, K., *et al.* (2019) High-resolution Raman microscopic detection of follicular thyroid cancer cells with unsupervised machine learning. *J. Phys. Chem. B.* 123; 4358–4372.
 34. Tsuji, T., Matsuo, K., Nakahari, T., Marunaka, Y. and Yokoyama, T. (2016) Structural basis of the Inv compartment and ciliary abnormalities in *Inv/nphp2* mutant mice. *Cytoskeleton* 73; 45–56.
 35. Wang, T. Y., Nallamothe, B. K., Krumholz, H. M., Li, S., Roe, M. T., Jollis, J. G., *et al.* (2011) Association of door-in to door-out time with reperfusion delays and outcomes among patients transferred for primary percutaneous coronary intervention. *JAMA* 305; 2540–2547.
 36. Webster, K. A. (2012) Mitochondrial membrane permeabilization and cell death during myocardial infarction: roles of calcium and reactive oxygen species. *Future Cardiol.* 8; 863–884.
 37. Yamamoto, T., Minamikawa, T., Harada, Y., Yamaoka, Y., Tanaka, H., Yaku, H., *et al.* (2018) Label-free Evaluation of Myocardial Infarct in Surgically Excised Ventricular Myocardium by Raman Spectroscopy. *Sci. Rep.* 8; 14671.
 38. Yamazaki, S., Doi, K., Numata, S., Itatani, K., Kawajiri, H., Morimoto, K., *et al.* (2016) Ventricular volume and myocardial viability, evaluated using cardiac magnetic resonance imaging, affect long-term results after surgical ventricular reconstruction. *Eur. J. Cardiothorac. Surg.* 50; 704–712.
 39. Zhang, Z. M., Chen, S., Liang, Y. Z., Liu, Z. X., Zhang, Q. M., Ding, L. X., *et al.* (2010) An intelligent background-correction algorithm for highly fluorescent samples in Raman spectroscopy. *J. Raman Spectrosc.* 41; 659–669.